Journal of Alloys and Compounds 509 (2011) 7595–7599

Contents lists available at ScienceDirect

Journal of Alloys and Compounds

journal homepage: www.elsevier.com/locate/jallcom

Thermo-electrochemical activation of Cu_3Sn negative electrode for lithium-ion batteries

Ji Y. Kwon [a], Ji Heon Ryu [b], Yoon S. Jung [a,1], Seung M. Oh [a,*]

[a] Department of Chemical and Biological Engineering and WCU Program of C_2E_2, Seoul National University, 599 Gwanangno, Gwanak-gu, Seoul 151-744, Republic of Korea
[b] Graduate School of Knowledge Based Technology and Energy, Korea Polytechnic University, Siheung, Gyeonggi 429-923, Republic of Korea

ARTICLE INFO

Article history:
Received 16 December 2010
Received in revised form 10 April 2011
Accepted 11 April 2011
Available online 20 April 2011

Keywords:
Lithium-ion batteries
Cu–Sn intermetallic compounds
Thermo-electrochemical activation
Lithiation
De-lithiation

ABSTRACT

A Cu_3Sn film electrode (thickness = *ca.* 3 μm) is prepared by DC magnetron sputtering deposition of Sn on Cu substrate and subsequent annealing at 300 °C for 30 h. At 25 °C, this Cu–Sn binary intermetallic compound is inactive for lithiation, but becomes active at elevated temperatures due to facilitation of Cu–Sn bond cleavage for the conversion-type lithiation. The lithiated product at 120 °C is the most Li-rich Li–Sn alloy ($Li_{17}Sn_4$). Upon de-lithiation, the Cu–Sn intermetallics of different compositions are generated by the reaction between the metallic Sn that is restored from $Li_{17}Sn_4$ and the idling metallic Cu. The nature of the resulting intermetallics is dependent on the de-lithiation temperature: $Cu_{10}Sn_3$ at 120 °C and Cu_6Sn_5 at 25 °C. Only the latter is active for lithiation in the subsequent room-temperature cycling. That is, Cu_3Sn is thermo-electrochemically activated to be Cu_6Sn_5 by lithiation at 120 °C and subsequent de-lithiation at 25 °C. The higher lithiation activity observed with the more Sn-rich phase (Cu_6Sn_5) compared to the initial one (Cu_3Sn) has been accounted for by the higher equilibrium lithiation potential (thermodynamic consideration) and smaller number of Cu–Sn bonds to be broken (kinetic consideration).

1. Introduction

The Li-alloying materials (for instance, Si and Sn) have attracted much attention as one of the promising alternatives to the carbon-based negative electrodes for lithium-ion batteries. Their theoretical capacity ($Li_{15}Si_4$: 3579 mA h g^{-1} and $Li_{17}Sn_4$: 960 mA h g^{-1}) is much higher than that of already-commercialized graphite (372 mA h g^{-1}). One of the critical problems encountered with these Li-alloying electrodes is, however, the massive volume change evolving during the alloying and de-alloying reaction with Li. The repeated volume change frequently leads to a pulverization of the Li-alloying materials themselves and break-down of the electrically conductive network within the electrode layers [1–3]. To overcome or at least alleviate this volume-change problem, at least two approaches have been made. First, the Li-alloying materials are loaded into the electrode layers as nano-sized powders [3–7]. The underlying idea for this nano-size approach is that the pulverization can be alleviated since the absolute volume change becomes smaller by virtue of a decrease in the particle size. This nano-size approach is, however, partially successful in that such small particles are aggregated to be larger ones during alloying and de-alloying period, then pulverized again [8,9]. The second approach is to formulate the Li-alloying materials into active/inactive intermetallic compounds (*AB*), where *A* is the Li-alloying materials (Si, Sn, Sb, Al, Ga and In) and *B* is the metallic components that are inactive for lithiation reaction (Cu, Fe, Ni, Co, Ti, and Mn) [5,10–19]. Recently, an excellent review on the active/inactive intermetallic compounds has been provided in Ref. [19]. The key idea for this approach is that the inactive metallic component (*B*) plays a buffering role against the massive volume change encountered in the active component (*A*). Indebted to this buffering role, the cycle performances of the Li-alloying electrodes can be improved in many binary intermetallic compounds [10–18]. Nonetheless, the previous literatures complain that the active components (Li-alloying materials) are still inactive for lithiation or show a much lower capacity than the theoretical values at room temperature, even if they are formulated into binary intermetallic compounds; Cu_3Sn [13,20], Cu_3Si [21], Ni_xSi [22] and Al–M (M = Cr, Fe, Mn and Ni) [23,24]. Such a slow kinetics seems to be due to a high activation energy needed for *A*–*B* bond cleavage since the active components (*A*) can be lithiated after the bond cleavage. A simple measure to enhance the lithiation activity of these materials may thus be the elevation of working temperature.

In our previous work [25], the last approach has been tested on a Cu–In binary intermetallic compound (Cu_7In_3) that is inactive for lithiation at room temperature. As expected, the Cu_7In_3 electrode showed a lithiation behavior at elevated temperatures (55–120 °C). Namely, Cu_7In_3 was converted, upon lithiation, to a mixture of

* Corresponding author. Tel.: +82 2 880 7074; fax: +82 2 872 5755.
E-mail addresses: seungoh@snu.ac.kr, seungoh@plaza.snu.ac.kr (S.M. Oh).
[1] Present address: National Renewable Energy Laboratory, Golden, CO 80401, USA.

0925-8388/$ – see front matter © 2011 Elsevier B.V. All rights reserved.
doi:10.1016/j.jallcom.2011.04.060

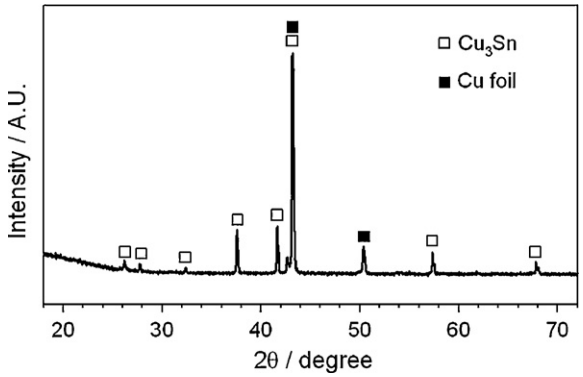

Fig. 1. XRD pattern obtained with the Cu_3Sn film electrode. The XRD pattern is indexed with Cu_3Sn (PDF# 00-001-1240).

nano-sized metallic Cu and In grains through the Cu–In bond cleavage, and the resulting In component was lithiated. Two important observations were made there. First, the more In-rich phase (CuIn) was generated upon de-lithiation through the reaction between the inactive Cu and elemental In that was restored from the lithiated In phases (Li_xIn). Second, the as-generated CuIn phase was then active for lithiation at room temperature. This phenomenon has been named "thermo-electrochemical activation" since the room-temperature inactive phase (Cu_7In_3) is converted to an active one (CuIn) by electrochemical reaction at elevated temperatures.

This work is an extension of the previous one. Here, thermo-electrochemical activation of Cu_3Sn, which is also inactive for lithiation at room temperature, is examined with three major concerns in mind: (i) if the room-temperature inactive Cu_3Sn phase becomes active at elevated temperatures or not, (ii) if this binary intermetallic compound is thermo-electrochemically activated or not, and (iii) if this is the case, which Cu–Sn phases are generated by the thermo-electrochemical activation.

2. Experimental

The Cu_3Sn film electrode was prepared by DC magnetron sputtering of Sn (99.99%, Applied Science Corp.) on a piece of Cu foil (thickness = 25 μm) and annealing at 300 °C for 30 h under vacuum. The deposition was made under an Ar atmosphere (5.0 mTorr). The thickness of Cu_3Sn layer, estimated by field-emission scanning electron microscopy (FE-SEM, JEOL JSM-6700F), was 3 ± 0.3 μm when the power was 0.94 kW and the sputtering time was 60 s.

A coin-type electrochemical cell (2032-type) was fabricated using Li foil as the counter electrode and a glass fiber sheet as the separator. The used electrolyte was 1.0 M LiBOB (lithium(bis)oxaloborate) dissolved in GBL (γ-butyrolactone). Galvanostatic discharge/charge cycling was made at a current density of 100 mA g_{Sn}^{-1} in the potential range of 0.0–2.0 V (vs. Li/Li^+). Here, the current density was calculated on the basis of the weight of Sn in Cu_3Sn.

Phase transitions evolved during the thermo-electrochemical activation were traced by using X-ray diffraction (XRD) analysis. The XRD patterns were obtained using a Rigaku diffractometer equipped with a CuKα radiation (λ = 1.541 Å). For the XRD analysis, the cells were disassembled and the Cu_3Sn film electrodes were washed with dimethyl carbonate (DMC) and dried. The samples were sealed with a beryllium window, the backside of which was sealed by kapton tape in an Ar-filled dry box to avoid air contact.

Cycling performance of the thermo-electrochemically activated Cu_3Sn electrodes was compared with that of a pure Sn film electrode. The Sn film was sputter deposited on Mo substrate that is not alloying with Sn. The deposition time was extended to 150 s to obtain a comparable weight of Sn on the Mo substrate to that on the Cu foil. The weight of Sn was determined by weighing the electrodes before and after the Sn deposition. In this report, lithiation was expressed as discharging, whereas de-lithiation as charging based on the standard lithium-ion cell configuration.

3. Results and discussion

Fig. 1 shows the X-ray diffraction (XRD) pattern obtained with the Cu_3Sn film electrode prepared by the DC magnetron sputtering. The diffraction peaks belonging to metallic Cu are easily recognized.

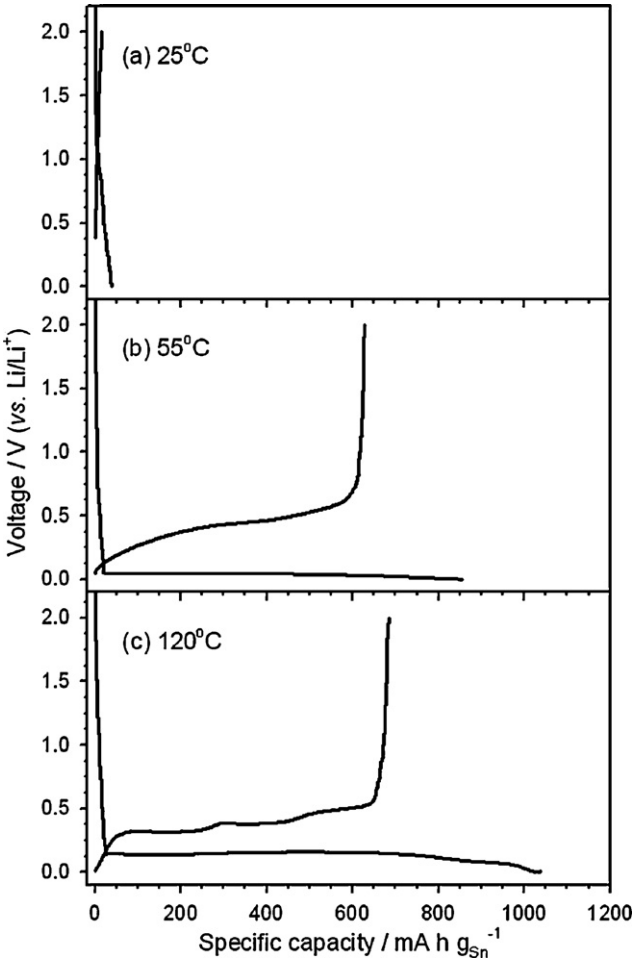

Fig. 2. The first galvanostatic discharge–charge voltage profiles obtained with Cu_3Sn/Li cell as a function of working temperature. Voltage cut-off = 0.0–2.0 V (vs. Li/Li^+). Current density = 100 mA g_{Sn}^{-1}.

The other diffraction peaks are well-matched with those for Cu_3Sn, except that the relative peak intensity is somewhat different to that of the powder samples, probably due to a preferred orientation of Cu_3Sn grains [26].

The first concern in this work is to see if or not the room-temperature inactive Cu_3Sn phase becomes active at elevated temperatures. The galvanostatic discharge (lithiation) and charge (de-lithiation) voltage profiles obtained with the Cu_3Sn/Li cell are presented in Fig. 2, in which the working temperature is indicated in the inset. At 25 °C, the cell shows a negligible lithiation activity in accordance with the previous report [13]. When the working temperature is raised, however, the lithiation reaction is indeed occurring. The lithiation capacity becomes larger with an increase in the working temperature to deliver a value of 1050 mA h g_{Sn}^{-1} at 120 °C. Three features should be noted in Fig. 2. First, the lithiation voltage profiles obtained at the elevated temperatures show a long plateau near 0.0 V (vs. Li/Li^+), which is the characteristic feature for the conversion-type lithiation reaction [27]. This illustrates that the Cu–Sn bonds in Cu_3Sn are broken for the Sn component to be lithiated. Second, the lithiation voltage plateau at 120 °C (*ca.* 0.2 V vs. Li/Li^+) appears earlier than that observed at 55 °C (*ca.* 0.05 V), reflecting that the overpotential required for the Cu–Sn bond cleavage is smaller at higher temperature. Third, at least three voltage plateaus are discernable in the de-lithiation voltage profile obtained at 120 °C. Given that the similar voltage plateaus are observed with pure Sn electrodes [28], it is sure that the Li–Sn alloys (Li_xSn) are formed upon lithiation and they are de-lithiated with

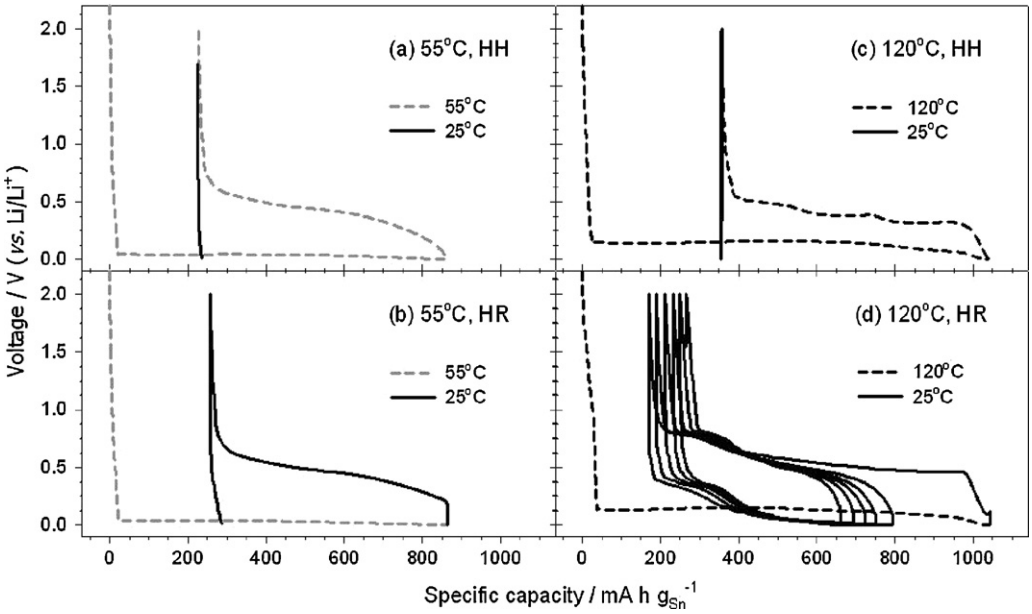

Fig. 3. Thermo-electrochemical activation behavior of the Cu_3Sn film electrode. Voltage cut-off = 0.0–2.0 V (vs. Li/Li^+). Current density = 100 mA g_{Sn}^{-1}. Note that only the sample activated by HR scheme at 120 °C/25 °C (d) shows a lithiation activity at room temperature.

the characteristic voltage plateaus. In short, the room-temperature inactive Cu_3Sn electrode becomes active for lithiation since the Cu–Sn bond cleavage is facilitated by raising the working temperature.

The second concern in this work is to see if the Cu_3Sn electrode is thermo-electrochemically activated or not. To test this possibility, the activation is tried by two schemes and the room-temperature lithiation activity is examined thereafter. In the first activation scheme, lithiation is made at elevated temperatures but de-lithiation at room temperature (HR scheme). In the other scheme, both lithiation and de-lithiation are made at elevated temperatures (HH scheme). When the Cu_3Sn film electrode is lithiated/de-lithiated at 55 °C (dotted line in Fig. 3a), it does not show any lithiation activity in the subsequent room-temperature cycling (solid line in Fig. 3a). The Cu_3Sn film electrode that is lithiated at 55 °C and de-lithiated at 25 °C also gives negligible activity in the forthcoming lithiation period at 25 °C (Fig. 3b). The electrode activated according to the HH scheme at 120 °C still does not show any activity at room temperature (Fig. 3c). Only the Cu_3Sn electrode lithiated at 120 °C and de-lithiated at 25 °C shows a lithiation and de-lithiation activity at room temperature (Fig. 3d). That is, only the last trial is successful for thermo-electrochemical activation.

It is curious that the HR scheme made at 120 °C/25 °C works for the activation (Fig. 3d), but the HH scheme made at 120 °C/120 °C does not (Fig. 3c). To solve this, the phase evolution occurring in the activation period is traced by using XRD technique. Fig. 4a presents the voltage profiles obtained with the two activation schemes, in which the points where the XRD measurements were made are indicated. The XRD pattern obtained after the Cu_3Sn electrode is lithiated down to 0.0 V at 120 °C (*i*) is shown in Fig. 4b. The diffraction peaks are well matched with those of $Li_{17}Sn_4$ ($Li_{4.25}Sn$), indicating that the Sn component in Cu_3Sn is lithiated up to the most Li-rich phase. The most Li-rich Li–Sn alloy was once considered as $Li_{22}Sn_5$ ($Li_{4.4}Sn$), but fixed as $Li_{17}Sn_4$ ($Li_{4.25}Sn$) by the later re-examination [29]. The following conversion-type lithiation reaction can thus be assumed at 120 °C:

$$4\,Cu_3Sn + 17\,Li^+ + 17\,e^- \rightarrow Li_{17}Sn_4 + 12\,Cu \quad (1)$$

The phases evolved after the HH scheme at 120 °C give some sharp and distinct diffraction peaks (*ii*), whereas the HR scheme gives some weak and broad peaks (*iii*). The phases generated at (*ii*) and (*iii*) are not identical since the XRD patterns differ to each other. Identification of these two phases is difficult since the number of diffraction peaks is limited and the peaks are broad. Another difficulty in phase identification is that the phase evolution may be incomplete or controlled by kinetic variables (current density and upper cut-off voltage) since the samples are cycled in a transient (dynamic) condition. To overcome this, the electrode potential was held at (*ii*) and (*iii*) for two days to obtain the quasi-equilibrium phases. The quasi-equilibrium phases evolved at (*ii*) and (*iii*) turn out to be $Cu_{10}Sn_3$ (Fig. 5a) and Cu_6Sn_5 (Fig. 5b), respectively. These XRD patterns are not far different to those obtained under the transient condition (Fig. 4b). Namely, the three most intense peaks at 24.0°, 42.2° and 61.9° on (*ii*) in Fig. 4b also appear in Fig. 5a. The most intense peak at 30.1° in Fig. 5b is also found at (*iii*) in Fig. 4b. The absence of other diffraction peaks and mismatches in the peak intensity may be caused by an incomplete phase formation in the transient experiment (Fig. 4). The XRD data obtained at (*iv*) is also displayed in Fig. 4b. The broad peak at 19–24° in (*iv*) can be correlated with the three peaks located at the same region in (*i*), whereas the broad peak at *ca.* 38° in (*iv*) corresponds to that appeared at the same angle in (*i*). This illustrates that the lithiated phase evolved at (*iv*) in Fig. 4a is the same as that generated at (*i*). That is, the electrochemically activated electrode is also lithiated to the most Li-rich phase ($Li_{17}Sn_4$) at room temperature.

A question arises as to why the Cu–Sn intermetallic phase generated by HR scheme (Cu_6Sn_5) is active for lithiation at room temperature (Fig. 3d), while that generated by HH scheme ($Cu_{10}Sn_3$) is not (Fig. 3c). The answer may be found from the fact that the former is more Sn-rich than the latter. A literature survey on the binary intermetallic compounds (*AB*, where *A* is the Li-alloying materials and *B* is the inactive metallic component) reveals that the more *A*-rich compounds show a higher lithiation activity [30–33]. For instance, the lithiation activity increases with an increase in the In content in the Cu–In and Ni–In binary intermetallic compounds [25]. The lithiation activity shows the following increasing order; $Cu_7In_3 < Cu_{11}In_9 < CuIn$ and $Ni_3In < Ni_2In_3$. This observation can be rationalized on the basis of both thermodynamic and kinetic considerations. The equilibrium lithiation potential can

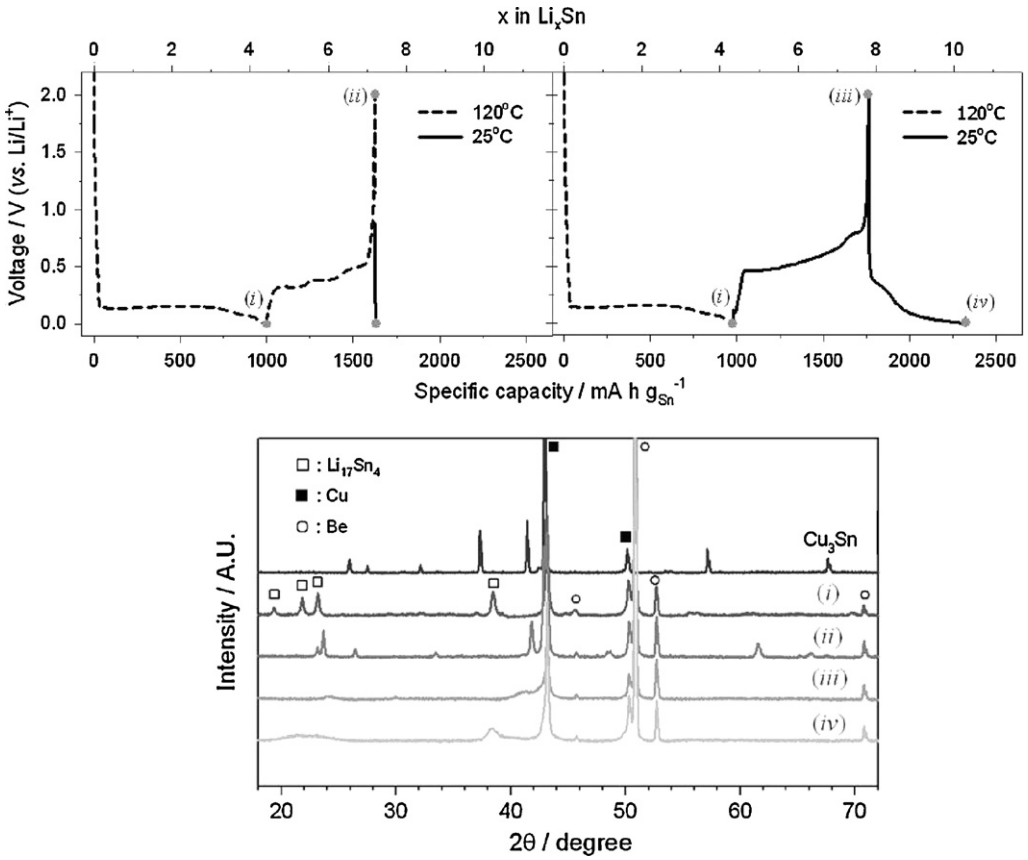

Fig. 4. (a) Galvanostatic discharge–charge voltage profiles with the points where XRD measurements were made. (b) XRD patterns obtained at the points shown in (a). The diffraction peaks obtained at (*i*) are indexed with those of $Li_{17}Sn_4$ (PDF# 01-070-9404).

be expressed by Eq. (2).

$$E_2^\circ = E_1^\circ + \frac{\Delta G_f^\circ(AB_x)}{nF} \quad (2)$$

Here E_1° and E_2° are the equilibrium lithiation potentials for pure *A* and AB_x intermetallic compounds, respectively. The free energy formation (ΔG_f°) has a negative value for AB_x, such that $E_1^\circ > E_2^\circ$. This indicates that the lithiation of AB_x intermetallic compounds is thermodynamically less favored than that for the pure active *A*. When the equilibrium lithiation potentials are compared for AB_x intermetallic compounds of different composition, the more *A*-rich ones show more positive values as they have less negative ΔG_f° per mole of AB_x [23,34], such that the lithiation is thermodynamically more feasible with the more *A*-rich ones. From a kinetic consideration, the more *A*-rich intermetallic compounds should have higher reactivity because they have fewer *A*–*B* bonds to be broken. That is, the extreme of *A*-rich intermetallic compound (pure *A*, pure Sn in this work) does not have *A*–*B* bonds to be broken, thereby it shows a higher lithiation activity than AB_x intermetallic compounds (Cu_3Sn, $Cu_{10}Sn_3$ and Cu_6Sn_5 in this work).

Finally, the cycle performance of thermo-electrochemically activated Cu_3Sn electrode is compared to that of a pure Sn electrode at room temperature (Fig. 6). As seen, the thermo-electrochemically

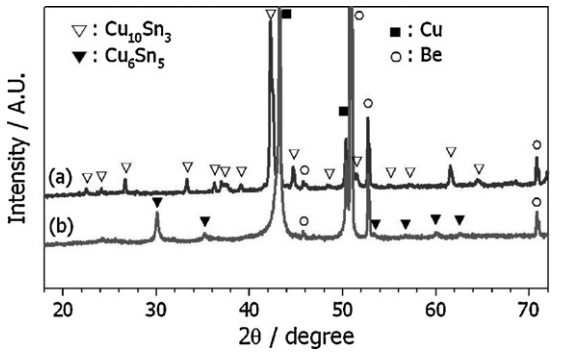

Fig. 5. The XRD patterns obtained after the electrode was held at 2.0 V for two days at (*ii*) and (*iii*) in Fig. 4a. The diffraction peaks are indexed with those of $Cu_{10}Sn_3$ (PDF# 00-026-0564) and Cu_6Sn_5 (PDF# 00-045-1488).

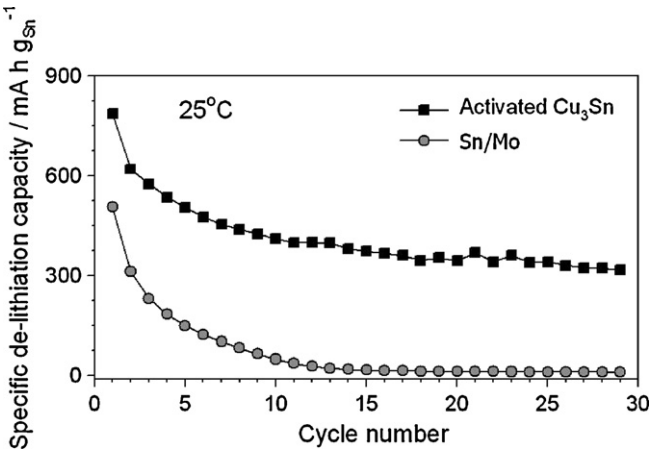

Fig. 6. The room-temperature (25 °C) cycle performance observed with the thermo-electrochemically activated Cu_3Sn (actually Cu_6Sn_5) and the pure Sn electrode. For comparison, the weight of deposited Sn was controlled to be the same for both electrodes. Current density = 100 mA g_{Sn}^{-1}.

activated electrode (Cu_6Sn_5) shows a better cycling performance compared to the pure Sn electrode. The pure Sn electrode fails within a few cycles, which must be due to a pulverization of Sn and break-down of electrically conductive network. The better cycle performance observed with the thermo-electrochemically activated electrode (Cu_6Sn_5) must be indebted to the presence of Cu that serves as a buffer against the volume change of the Sn component.

4. Conclusions

Thermo-electrochemical activation behavior of Cu_3Sn film electrode is examined with three major concerns in mind. The following points of value may be gleaned on the three issues raised in Introduction section.

(i) A Cu_3Sn film electrode is prepared on Cu substrate. This binary intermetallic compound is inactive for lithiation at room temperature, but becomes more active with an increase in the working temperature.
(ii) The Cu_3Sn phase is converted to $Li_{17}Sn_4$ upon lithiation at 120 °C, which is the most Li-rich phase in Li–Sn system. When the electrode is de-lithiated at 25 °C, the Cu_6Sn_5 phase is generated by the reaction between the restored Sn and idling Cu. The resulting Cu_6Sn_5 phase now shows a high lithiation activity even at room temperature. That is, the room-temperature inactive Cu_3Sn phase is converted to the active Cu_6Sn_5 by the thermo-electrochemical activation.
(iii) The Cu_6Sn_5 phase shows a higher lithiation activity than Cu_3Sn. This is consistent with the previous observation, in which the lithiation activity is higher with an increase in the active component (*A*) in *A*–*B* intermetallic compounds.

Acknowledgement

This work was supported by the WCU program through the National Research Foundation of Korea funded by the Ministry of Education, Science and Technology (R31-10013).

References

[1] R.A. Huggins, J. Power Sources 81–82 (1999) 13.
[2] M. Wachtler, J.O. Besenhard, M. Winter, J. Power Sources 94 (2001) 189.
[3] L.F. Nazar, G. Goward, F. Leroux, M. Duncan, H. Huang, T. Kerr, J. Gaubicher, Int. J. Inorg. Mater. 3 (2001) 191.
[4] J. Yang, M. Winter, J.O. Besenhard, Solid State Ionics 90 (1996) 281.
[5] U. Kasavajjula, C. Wang, A.J. Appleby, J. Power Sources 163 (2007) 1003.
[6] B. Guo, J. Shu, K. Tang, Y. Bai, Z. Wang, L. Chen, J. Power Sources 177 (2008) 205.
[7] Z. Zhou, Y. Xu, W. Liu, L. Niu, J. Alloys Compd. 493 (2010) 636.
[8] H. Li, L. Shi, W. Lu, X. Huang, L. Chen, J. Electrochem. Soc. 148 (2001) A915.
[9] H. Li, Q. Wang, L. Shi, L. Chen, X. Huang, Chem. Mater. 14 (2001) 103.
[10] L. Fang, B.V.R. Chowdari, J. Power Sources 97–98 (2001) 181.
[11] A. Bonakdarpour, K.C. Hewitt, R.L. Turner, J.R. Dahn, J. Electrochem. Soc. 151 (2004) A470.
[12] H. Mukaibo, T. Momma, M. Mohamedi, T. Osaka, J. Electrochem. Soc. 152 (2005) A560.
[13] J. Park, S. Rajendran, H. Kwon, J. Power Sources 159 (2006) 1409.
[14] X. Fan, Q. Zhuang, H. Jiang, L. Huang, Q. Dong, S. Sun, Acta Phys. Chim. Sin. 23 (2007) 973.
[15] A.D.W. Todd, P.P. Ferguson, M.D. Fleischauer, J.R. Dahn, Int. J. Energy Res. 34 (2010) 535.
[16] X. Wang, Z. Wen, Y. Liu, L. Huang, M. Wu, J. Alloys Compd. 506 (2010) 317.
[17] Y.-S. Lin, J.-G. Duh, H.-S. Sheu, J. Alloys Compd. 509 (2011) 123.
[18] W. Cui, F. Wang, J. Wang, H. Liu, C. Wang, Y. Xia, J. Power Sources 196 (2011) 3633.
[19] W.-J. Zhang, J. Power Sources 196 (2011) 13.
[20] L. Xue, Z. Fu, Y. Yao, T. Huang, A. Yu, Electrochim. Acta 55 (2010) 7310.
[21] J.-H. Kim, H. Kim, H.-J. Sohn, Electrochem. Commun. 7 (2005) 557.
[22] M.-S. Park, Y.-J. Lee, S. Rajendran, M.-S. Song, H.-S. Kim, J.-Y. Lee, Electrochim. Acta 50 (2005) 5561.
[23] D. Larcher, L.Y. Beaulieu, O. Mao, A.E. George, J.R. Dahn, J. Electrochem. Soc. 147 (2000) 1703.
[24] M.D. Fleischauer, M.N. Obrovac, J.D. McGraw, R.A. Dunlap, J.M. Topple, J.R. Dahn, J. Electrochem. Soc. 153 (2006) A484.
[25] Y.S. Jung, K.T. Lee, J.H. Kim, J.Y. Kwon, S.M. Oh, Adv. Funct. Mater. 18 (2008) 3010.
[26] K.H. Prakash, T. Sritharan, Acta Mater. 49 (2001) 2481.
[27] J.-M. Tarascon, S. Grugeon, M. Morcrette, S. Laruelle, P. Rozier, P. Poizot, C. R. Chimie 8 (2005) 9.
[28] M. Inaba, T. Uno, A. Tasaka, J. Power Sources 146 (2005) 473.
[29] G.R. Goward, N.J. Taylor, D.C.S. Souza, L.F. Nazar, J. Alloys Compd. 329 (2001) 82.
[30] O. Mao, J.R. Dahn, J. Electrochem. Soc. 146 (1999) 423.
[31] J.R. Dahn, R.E. Mar, A. Abouzeid, J. Electrochem. Soc. 153 (2006) A361.
[32] J.-j. Zhang, Y.-y. Xia, J. Electrochem. Soc. 153 (2006) A1466.
[33] A.D.W. Todd, R.E. Mar, J.R. Dahn, J. Electrochem. Soc. 153 (2006) A1998.
[34] F.R. de Boer, Cohesion in Metals: Transition Metal Alloys, North-Holland, Elsevier Scientific Pub. Co, Amsterdam, New York, 1988, p. 310.